PAPER AAS 96-152

ADAPTIVE ORBIT DETERMINATION FOR INTERPLANETARY SPACECRAFT

P. Daniel Burkhart
Robert **H. Bishop**

Jet Propulsion Laboratory
California Institute of Technology
Pasadena, California

AAS/AIAA Space Flight Mechanics Meeting

Austin, Texas **12-15 February 1996**

AAS Publications Office, P.O. Box 28130, San Diego, CA 92198

AAS 96-152

ADAPTIVE ORBIT DETERMINATION FOR INTERPLANETARY SPACECRAFT

P. Daniel Burkhart* **Robert H. Bishop†**

The interplanetary orbit determination problem has been traditionally solved, using least-squares techniques. Due to operational limitations of this method, a Kalman filter approach has been proposed for future missions which includes all spacecraft and measurement modeling states in the filter. The goal is to increase the accuracy of the navigation process while utilizing only radiometric (Doppler and range) data. As an extension, an adaptive orbit determination approach (based on the Magill filter bank) has been developed here to process radiometric data. This adaptive approach can be used to systematically determine the operational filter parameters, which are currently selected using *ad hoc* methods. The Mars Pathfinder mission is utilized to demonstrate the effectiveness of the adaptive filter bank in determining variances for the process and measurement noise parameters based on the tracking data. Results for the range case show that the adaptive enhanced filter bank is effective in selecting the noise variances that match those used to generate the data. Results for the Doppler case are not as conclusive, due primarily to linearization errors.

INTRODUCTION

The orbit determination problem for interplanetary spacecraft involves the calculation of spacecraft states (i.e. position and velocity) and associated estimation uncertainty measures based on information received from measurements that are corrupted by various errors and random noise. One problem with the current approach to solving this problem is the lack of a systematic method for determining appropriate values for the operational orbit determination filter. The operational filter parameters, such as time constants, gravitational parameters, noise variances and system parameters, are generally selected by trial and error based on *experience* and *computer simulation.* A set of filter parameters are selected and the measurement data is processed_. Based on the simulation results, the filter parameters may

*Member Technical Staff, Navigation and Flight Mechanics Section, Jet Propulsion Laboratory, California Institute of 'Ike.hnology, Pasadena, CA 91109; Member AIAA.

†Associate Professor, Department of Aeroepace Engineering and Engineering Mechanics, The University of Texas, Austin, Texas 7S712; Member AlAA.

be changed and the data processed again, or the current result maybe accepted. During this iterative process, often the measurement data is de-weighted, resulting in estimation errors that are generally higher than the data requires. This *ad hoc* approach to filter tuning, in addition to failing to take full advantage ofthe inherent" "data accuracy, requires a large number of navigation team members to analyze the results. Despite the success of this approach in the past, current realities do not support its continued use. The orbit determination task must be completed with fewer analysts due to reductions in resources for navigation, similar if not greater tracking accuracy requirements, and less tracking data.

In addition to the systematic tuning of the operational filter, an approach for detecting environmental changes is desirable. Suppose the process noise and/or data noise profile changes during the mission. For example, the acceleration profile of the spacecraft may change significantly due to unmodeled venting. The need for a non-labor intensive method to detect changes in the data profile and to point to the source of the changes is clear (e.g. detect an unmodeled vent) .

For these reasons, a new orbit determination methodology is desirable for operational interplanetary navigation. The motivation for the work presented here is to improve the operational tools used to perform the interplanetary orbit determination function.

One constraint on the proposed solution is the utilization of *realistic* error sources and *realistic* models to accurately determine if the proposed approach will be useful in an operational environment. In addition, the proposed solution must integrate easily with current navigation approaches. Since a Kalman filter approach will be used for future interplanetary missions, the solution must be compatible with this recursive filter method. Due to the desire to minimize tracking station use, personnel costs and complexity, only conventional Doppler and ranging data will be considered. Finally, the proposed solution must be implementable in a modular fashion. This is not only to avoid extensive modification of existing orbit determination software, but also to allow testing and verification in a smoother and less complicated fashion.

Along with the change from the least-squares filter to the Kalman filter, another major change in the current filtering practice is reflected in the so-called *enhanced filter*[1]. Current practice involves modeling certain Earth platform and transmission media effects as *consider parameters* in the filter, In other words, these parameters are allowed to affect the covariance of the estimated state, but are not themselves estimated. The enhanced filter calls for inclusion of all these parameters in the estimated state vector. In other words, the enhanced filter has no consider parameters. When compared with current filtering practices, the result is increased accuracy in the state estimates[1]. This filtering strategy is currently being tested using actual flight data from Galileo[2]. The enhanced Kalman filter is utilized in this paper.

The scenario chosen for this study is the Mars Pathfinder mission, scheduled for launch in December 1996, Specifics of the mission plan, including launch and arrival dates and the tracking scenario, are presented, A model was developed to represent accurately, but with moderate complexity, the actual data received by

the filter during a mission. This model, consisting of the spacecraft state, solar radiation pressure effects, small unmodeled acceleration effects, transmission media effects and Earth platform effects, is used to generate tracking data.

The approach taken here is to utilize radiometric (Doppler and range) data and to establish navigation improvements through the use of *adaptive filtering* algorithms. Several methods were investigated in terms of ability to determine both process noise and measurement noise parameters and to be general enough to handle a time-varying problem. Since the Kalman filter is already in use and is planned for future use for orbit determination, a method utilizing this approach is desirable for implementation reasons. It was found that the most desirable approach, in terms of these constraints, is the Magill Kalman filter bank[3], also known as the Multiple Model Estimation Algorithm (MMEA).

Results are given for several different sets of noise parameters included in the adaptive scheme. The main result is the demonstrated ability of the adaptive Kalman filter bank to determine the underlying measurement and process noise strengths. In addition, the results for the changing noise strengths case show the ability of the filter bank to detect environmental and/or spacecraft changes.

Following this introduction is the Mars Pathfinder mission description, with details on the adaptive filtering approaches and the Kalman filter bank next, The simulation results, followed by conclusions and future directions, complete the paper.

MARS PATHFINDER MISSION

The Mars Pathfinder mission is the first of a series of low-cost rapid turnaround science missions from NASA's Discovery Program. This mission will serve primarily as a demonstration of key technologies and concepts for use in future missions to Mars using scientific landers. In addition, Pathfinder includes a significant science payload. Investigations of the Martian atmosphere, surface meteorology, surface geology and morphology, and the elemental composition of Martian rocks and soil are scheduled for Pathfinder. A free-ranging surface microrover is also part of the mission. This microrover will be deployed by Pathfinder to conduct technology related experiments and to serve as a mechanism for instrument deployment.

The mission is scheduled for the 1996 Mars launch opportunity, with a 30 day launch window beginning on December 5, 1996 and ending on January 3, 1997. The arrival date at Mars is fixed at July 4, 1997. The transfer time will vary from 212 days to 182 days, depending on the actual launch date. The trajectory used for this study corresponds to the January 3, 1997 launch date, Upon arrival at Mars on July 4, 1997, the spacecraft will perform a direct entry into the Martian atmosphere. To achieve a landing, a parachute is deployed along with a rocket braking system and an airbag system. After landing the primary surface operations begin, which includes deployment of the microrover[4].

The interplanetary transfer phase of the Mars Pathfinder mission is under investigation here. The adaptive filtering approach proposed for the interplanetary navigation problem is not dependent on the Mars Pathfinder mission. The Mars

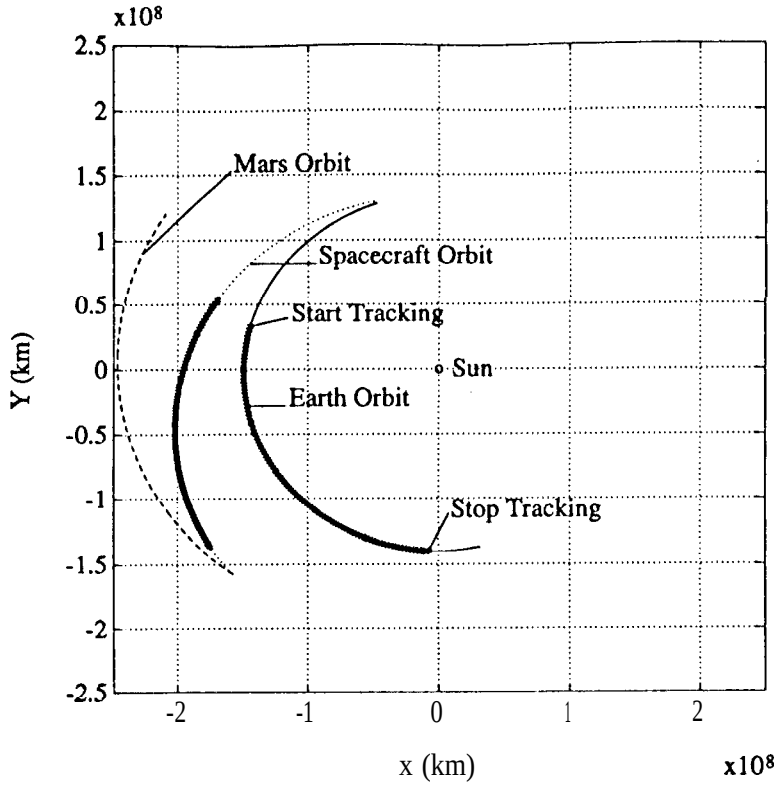

Figure 1 Mars Pathfinder Trajectory (planar projection)

Table 1
Mars Pathfinder trajectory characteristics (March 5-June 18, 1997)

Parameter	Value (start to end of arc)
Earth to spacecraft range (km)	36.2 X 10^6 to 180 × 10^6
Geocentric Declination (deg)	15.85 to –0.12
Sun-Earth-Probe (SEP) angle (deg)	1.4 to 51.7

Pathfinder scenario is chosen so that the adaptive filtering method can be tested using a realistic interplanetary mission. Epoch conditions are known for the spacecraft and the planets on March 5, 1997, The data arc used in this study lasts for 105 days from the epoch, or until June 18, 1997. A plot of the Earth, spacecraft and Mars trajectories is shown in Figure 1. The trajectory characteristics (the shaded portion of Figure 1) are detailed in Table 1. During interplanetary cruise, the scientific instruments will be checked but not used.

The interplanetary cruise portion of the mission begins approximately seven days after launch (L+7) and ends 15 days before encounter (M-15). The main task during

interplanetary cruise is to determine the required corrections to the trajectory to ensure the spacecraft arrives when and where it is scheduled. The nominal mission plan has four Trajectory Correction Maneuvers (TCM'S), if required. The first two maneuvers are scheduled at L+30 days (to correct for injection errors) and L+60 days (to correct remaining injection errors and TCM 1 errors). The third maneuver is scheduled for M-60 days (for entry targeting), while the final maneuver is planned for M-10 days (to insure the landing conditions are met). Thus the data arc used here begins after the completion of the first two TCM's and will include the third TCM. The solution at the end of data processing will be propagated to encounter, which includes the fourth TCM. The navigation solution, obtained after processing the data from the 105 day interplanetary cruise, will be used to support the final TCM if the maneuver is required. The errors due to the fourth TCM will not affect the navigation solution significantly

The tracking scenario contains two-way X/X band data taken from the Deep Space Network (DSN) 34-m High Efficiency (HEF) Deep Space Stations (DSSs) located near Goldstone, California (DSS 15), Canberra, Australia (DSS 45) and Madrid, Spain (DSS 65). The tracking schedule includes one pass of data for each station per week. The tracking passes are started with DSS 15 on the first day, DSS 45 on day four and DSS 65 on day six. After each station makes one pass, six passes (days) are skipped before the next pass at that station is initiated. Thus, DSS 15 will next track on day seven, DSS 45 on day ten and DSS 65 on day twelve. This pattern is repeated until the end of the considered portion of the trajectory. The interval between data points is ten minutes with range and Doppler data collected at the same time. The minimum elevation angles are 50° for DSS 15 and DSS 65, and 30° for DSS 45. Data points for times when the elevation angle is smaller than these values are rejected. All data points that meet the requirements for the day of the pass and the minimum elevation angle are included in the data set. These criteria were set in order to simulate the specified tracking schedule on one 4 hour pass per week at each tracking station during interplanetary cruise[4]. Following this schedule, about 1,250 range and 1, 250 Doppler measurements were available over the 105 day interplanetary cruise phase.

ADAPTIVE FILTERING APPROACHES

An implicit assumption in the Kalman filter is that all of the system parameters, including the state transition matrix, the measurement partial derivatives, and the process and measurement noise matrices are known. In general, this is not the case. Often there are parameters not included in the filter model that influence the measurements. This results in a modeling mismatch between the filter and the measurements which affects the state transition matrix and the measurement partials. In addition, the process noise and measurement noise matrices are rarely precisely known. For these reasons, it maybe desirable to apply an adaptive filtering scheme to the problem at hand.

The general problem to be solved is described by

$$\begin{aligned} z_{i+1} &= \Phi_i z_i + u_i \\ y_i &= H_i z_i + v_i \end{aligned}$$

where z_i is the state vector, Φ_i is the state transition matrix, u_i is the process noise vector, vi is the measurement noise vector and *Hi* is the measurement matrix. Both u_i and v_i are uncorrelated zero-mean Gaussian white noise sequences with

$$\begin{aligned} E\{u_i\} &= 0, & E\left\{u_i u_j^T\right\} &= Q\delta_{ij}, \\ \mathbf{E}\{v_i\} &= 0, & E\left\{v_i v_j^T\right\} &= R\delta_j, \end{aligned}$$

where Q is a nonnegative definite matrix and *R* is a positive definite matrix, both with unknown true values. The standard filtering problem is to estimate z_i based on the observation set $y_i^* = \{y_1, y_2, \ldots, y_i\}$, where the estimated values will be denoted $\hat{z}_i$. In this case, the discrete Kalman filter is used:

$$\begin{aligned} \hat{z}_{i+1}^{(-)} &= \Phi_i \hat{z}_i^{(+)} \\ P_{i+1}^{(-)} &= \Phi_i P_i^{(+)} \Phi_i^T + Q \\ \hat{z}_i^{(+)} &= \hat{z}_i^{(-)} + K_i \left(y_i - H_i \hat{z}_i^{(-)}\right) \\ K_i &= P_i^{(-)} H_i^T \left(H P_i^{(-)} H_i^T + R\right)^{-1} \\ P_i^{(+)} &= (I - K_i H_i) P_i^{(-)} \end{aligned}$$

where K_i is the Kalman gain and $\nu_i = y_i - H_i \hat{z}_i^{(-)}$ is the measurement residual with covariance $H P_i^{(-)} H_i^T + R$. This solution is optimal based on exact knowledge of Q and *R*. However, since this is not the case here, an adaptive filter will be used to help determine Q and *R*.

Evaluation of Adaptive Methods

Based on the discussion presented by Mehra in 1972, adaptive filtering methods can be divided into four groups: maximum likelihood, correlation, covariance matching and Bayesian[10]. Covariance matching techniques will not be discussed here.

A literature survey revealed several potential solutions to our problem. Computer experiments were conducted on the methods that showed the most promise[11]. A brief summary is presented here, Of the maximum likelihood methods, the one with a history in orbit determination was proposed by Meyers and Tapley[12]. However, this approach did not offer a significant improvement over current practice. Many correlation methods exist, but the most well-known was proposed by Mehra[13]. However, correlation methods are better suited to time-invariant problems. Attempts to extend this approach to time-varying problems have not been successful[14].

The Bayesian approach that isperhaps the most well-known is that originally formulated by Magill[3]. This method is known as simply the Kalman filter bank or the Multiple Model Estimation Algorithm (MMEA), shown in Figure 2[15]. The approach is to implement a bank of Kalman filters, each modeled with different values of a finite unknown parameter set. The method, in its original form, computes the weighted sum of the estimates from each filter to determine the optimal adaptive estimate.

The main reason the Kalman filter bank approach was selected here is that it solves the orbit determination problem quite well. The proposed methodology is also a practical extension to current navigation practices for interplanetary spacecraft. The cost of integrating this approach with the current operational enhanced Kalman filter is minimal. All that is required from the filter are pre-update measurement residuals and the covariance associated with these residuals at each data point, which are already computed by the Kalman filter. The assumptions that are required for application of the filter bank are the same that govern the use of a single Kalman filter. Thus, if the problem is formulated such that the Kalman filter is applicable, then the filter bank approach can be used without modification[16].

In addition, the filter bank approach has been shown to be a practical algorithm in solving real-world problems[17,18,19]. One important problem that can be solved most effectively using the Magill filter bank is that of hypothesis testing, which is to choose from among a finite set of filters the optimal filter in the bank[15,16]. In this use, the output of interest is the weight computed for each filter in the bank. The Kalman filter bank implemented in this study is utilized as a hypothesis tester.

The Kalman filter bank will allow the analyst to model several filters simultaneously and directly compare the results automatically. The filter bank will determine which filter is operating optimally (where optimal is precisely defined later) with respect to the measurement data, thus helping the process of selecting the filter parameters. For the case where the process and/or measurement noise profile changes, the filter bank can de-select a given filter and choose a different filter that more closely matches the current environment. In this way, in addition to the establishment of a systematic method to choose the operational filter parameters and to detect environmental changes, the orbit determination process can be completed with fewer team members, while potentially increasing the accuracy and timeliness of the results.

Adaptive Kalman Filter Bank Development

The problem to be solved may be stated as follows: An estimate is desired for a sampled-data, Gaussian process, which may be corrupted by additive noise, such that the estimate minimizes some performance measure. The observed process is a function of some unknown parameter vector, α, which is a member of a finite set of known parameter vectors[3].

Assume that the parameter vector α is a random variable that may or may not be Gaussian. This implies that α is an unknown constant for a specific sample run,

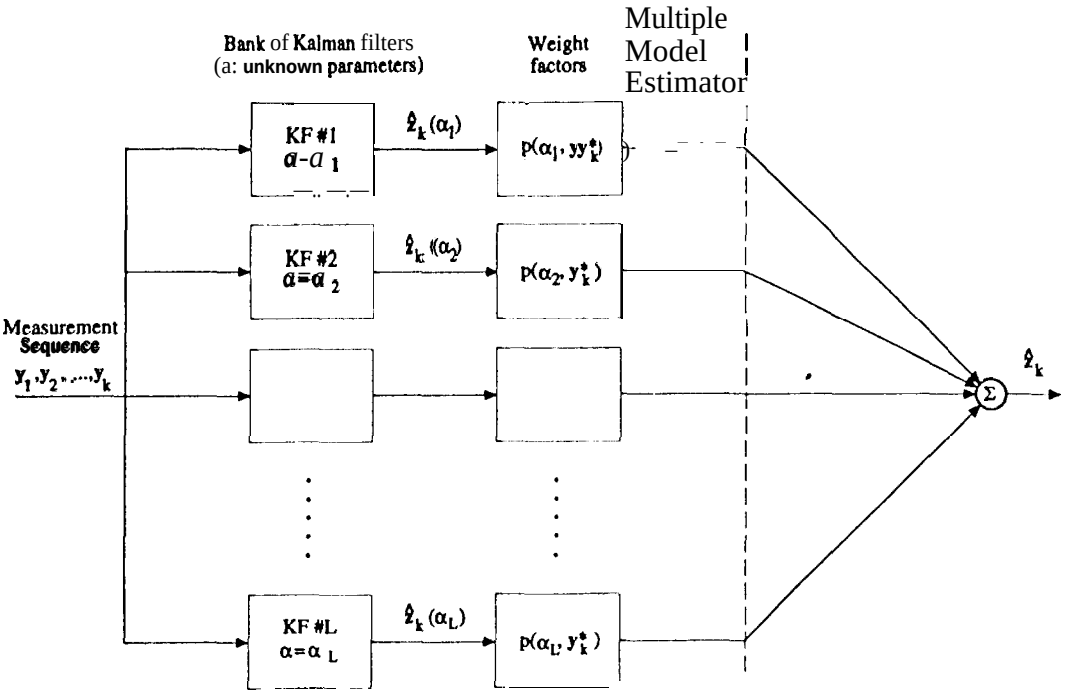

Figure 2 Weighted Sum of **Kalman** Filter Estimates

but has a known statistical distribution. The optimal estimate $\hat{z}_k$ is a weighted sum of the individual Kalman filters, with each filter operating with a different value of α. The weighted sum, for L Kalman filters, is given by

$$\hat{z}_k = \sum_{i=1}^{L} \hat{z}_k(\alpha_i) p(\alpha_i | y_k^*) \tag{1}$$

where $p(\alpha_i | y_k^*)$ is the discrete probability for α_i conditioned on the measurement sequence y_k^*. The problem now is reduced to the determination of the weight factors $p(\alpha_1 | y_k^*), p(\alpha_2 | y_k^*)$, etc. As the measurement process evolves, the weights change recursively. As more measurements are processed, the knowledge of the state and the unknown parameter α will increase. If as time progresses it is possible to learn which stochastic process is observed, then it is reasonable to expect the optimal estimator to converge to the appropriate filter for that process. In terms of the block diagram in Figure 2, the weighting coefficient for the true filter will converge to one while all of the rest will converge to zero[3,20].

The weighting factors $p(\alpha_i | y_k^*)$ are the adaptive feature of this estimator Using Bayes' rule, the weights are computed via

$$p(\alpha_i | y_k^*) = \left[\frac{p(y_k^* | \alpha_i) p(\alpha_i)}{\sum_{j=1}^{L} p(y_k^* | \alpha_j) p(\alpha_j)} \right], \qquad i = 1, 2, \ldots, L. \tag{2}$$

The values for $p(\alpha_i)$ are assumed known, so all the terms in this relation are known except for $p(y_k^* | \alpha_j)$. To compute the value for $p(y_k^* | \alpha_j)$, the processes x and y

will be assumed to be Gaussian. In addition, the measurement sequence $\boldsymbol{y}_k^*$ will be assumed to be a sequence of scalar measurements $y_0, y_1, \ldots, y_k$. When these conditions are applied, the result is

$$p(\boldsymbol{y}_k^*|\alpha_j) = \frac{1}{\sqrt{2\pi\left(\boldsymbol{H}_k\boldsymbol{P}_k^-\boldsymbol{H}_k^T + R_k\right)}} \exp\left[-\frac{1}{2}\frac{\left(y_k - \boldsymbol{H}_k\hat{\boldsymbol{z}}_k^-\right)^2}{\left(\boldsymbol{H}_k\boldsymbol{P}_k^-\boldsymbol{H}_k^T + R_k\right)}\right] p(\boldsymbol{y}_{k-1}^*|\alpha_j). \quad (3)$$

In general, $p(\boldsymbol{y}_k^*|\alpha_j)$ will be different for each filter in the bank.

In the Mars Pathfinder problem, only the *aposteriori* probabilities $p(\alpha_i|\boldsymbol{y}_k^*)$ for each hypothesis are computed by the filter bank. As the filter bank processes data, the weighting factor for the best filter will increase while the other weighting factors decrease[15]. For this problem, the Kalman filters are assumed to have an unknown measurement noise variance, in addition to possibly unknown process noise parameters. All other parameters and models between the filter and the environment are the same, Thus the MMEA will be determining the filter with the parameters that are the closest to the values from the environment, as determined from the measurements.

RESULTS

Results from several cases are shown. The first set of results are for the range case where all noise parameters are included in the filter, but only the measurement noise and NGA parameters are adaptively determined. In addition to the range case, a similar case where Doppler data is processed is shown. The final case involves a change in the nongravitational parameter during tracking. Range data is utilized in this study along with a high-gain antenna, which reduces the random noise component of the noise profile. This allows the Kalman filter bank to run over a larger set of data[11].

The models and values assumed for the error sources can be found in Table 2. Most are modeled as first-order Gauss-Markov random processes. The exceptions are the spacecraft state, with no associated process noise parameters, and the station locations, which are modeled as random biases with the variances shown in Table 2. The solar pressure model includes the symmetry of the spacecraft and the effect of the solar panels, and reflects a 5% uncertainty in the model parameters. The nongravitational accelerations approximate small unmodeled forces in each of the three coordinate directions due to gas leaks and attitude maintenance activity. The troposphere and ionosphere values are for each tracking station, The models are based on the Mars Pathfinder Operation Plan[4].

The results presented for each case include the estimates and the statistics for the orbit determination errors at the end of the tracking propagated to the nominal time of Mars encounter and expressed in terms of the B-plane coordinate frame[8]. This coordinate frame, also known as the aiming plane, is defined by unit vectors S, $\boldsymbol{T}$ and *R*. The vector S is parallel to the spacecraft velocity vector relative to

Table 2
Filter and Truth Model Parameters (one way)

Name	*a-priori* σ	steady-state σ	Time constant
Spacecraft State	10 km, 1 cm/s		
Solar Radiation Pressure:			
Radial (G_r)	5% (= 0.07)	5%	60 days
Transverse (G_x/G_y)	5% (= 0.02)	5%	60 days
Nongrav Accelerations:			
$(10^{-12}\ \mathrm{km/s^2})$	0.7	0.7	7 days
Station Locations:			
Spin axis	10 cm		
z-height	10 cm		
Longitude	10 cm		
Pole Orientation	10 cm (17 nrad)	10 cm	2 days
Rotation Period	15 cm (0.3225 ms)	15 cm	1 day
Zenith Troposphere	5 cm	5 cm	0.1 days
Zenith Ionosphere	3 cm (0.5 $\mathrm{el/m^2}$)	3 cm	0.2 day
Measurement Noise:			
Range	70 cm		
Doppler	O.O1 mm/see		

the target planet (Mars) at the time of entry into the target planet's gravitational sphere of influence, the vector T is perpendicular to the target planet equatorial plane and the vector R is such that the three unit vectors form a right handed coordinate system. The miss vector B is the aim point for planetary encounter and lies in the T-R plane. The miss vector would be the point of closest approach to the target planet ifthe target planet did not deflect the flight path of the spacecraft (i.e. the planet had no mass).

The statistics are presented as a l-u uncertainty of the miss vector resolved into miss components $B \cdot R$ (normal to the target planet equatorial plane) and $B \cdot T$ (parallel to the target planet equatorial plane), anda l-o uncertainty in the linearized time-of-flight (LTOF). The LTOF specifies the time of flight to encounter (point of closest approach) if the magnitude of the miss vector were zero and defines the time from encounter. The miss vector, or the distance from the center of Mars where the spacecraft crosses the target plane, is 4550 km oriented 201.8° clockwise from the T axis. In addition, the weighting coefficients for each filter in the bank are presented as a function of time.

The encounter plane error ellipse requirements (1σ) are 17 km for B o R, 6.2 km for B . T and 7 seconds for $LTOF$, with the error ellipse oriented at 111°4.

Results are not presented in this paper, due to space limitations, for the residuals and error covariances for the individual filters. These are useful in determining how well the filters are performing. The results obtained (but not shown here) show that the filter performance matches the computed weighting factors. In other words, filters with higher weights performed better than those with smaller weights.

Range Case

The first case considered adapts the nongravitational acceleration parameters and the measurement noise parameter. A bank of 15 filters is set up with the scaling from the nominal values as shown in Table 3. The filter numbers are determined as shown in the table. For example, filter 14 has a measurement noise that is ten times the nominal value and a NGA steady-state variance that is five times the nominal value.

The weighting factors for this scenario are plotted in Figure 3. This plot shows nonzero weights for filters 6, 7 and 8. The weight for filter 8 is nearly unity, while the other filters have negligible weights. The filters in the bank that do not have the correct measurement noise parameter are eliminated quickly by the MMEA. The remaining data is used to differentiate the process noise values from among the filters with the correct measurement noise parameter,

The encounter plane estimates and covariances for filters 6 through 10 are shown in Figure 4. For this case, filters 6 and 7 appear to be quite close to the truth. Filter 8, with a slightly higher weight and the correct filter, had slightly worse estimates. Since these results are based on a single realization of the random processes, Monte Carlo analysis with different realizations of the random processes was conducted to verify the expected results. The Monte Carlo results are presented in Burkhart[11].

Table 3
Scaling factors: Measurement and **NGA Parameters**

NGA Scaling	Filter Number		
0.1	1	6	11
0,2	2	7	12
1.0	3	8	13
5.0	4	9	14
10.0	5	10	15
	0.1	1.0	10.0
	Measurement Noise Scaling		

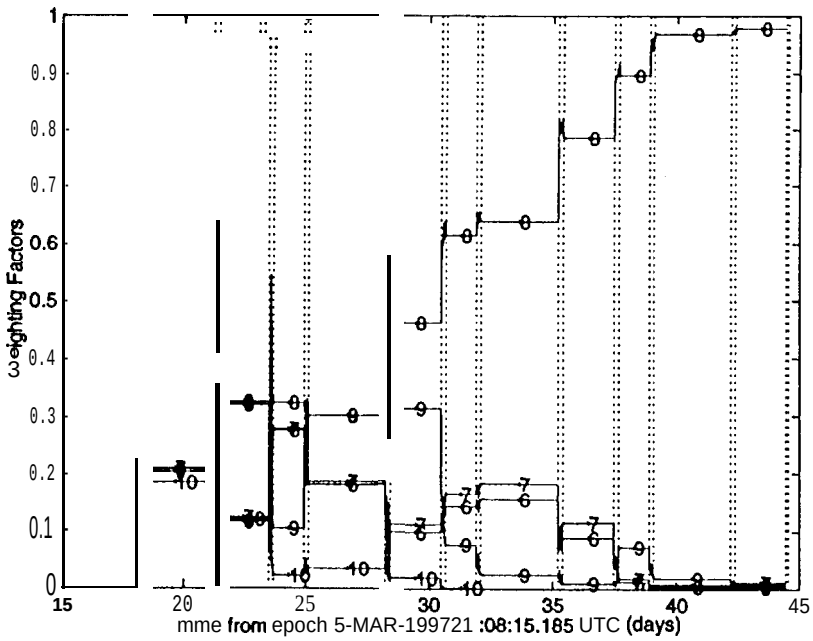

Figure 3 **Weighting Coefficients – Measurement and NGA Parameters Adapted (Range)**

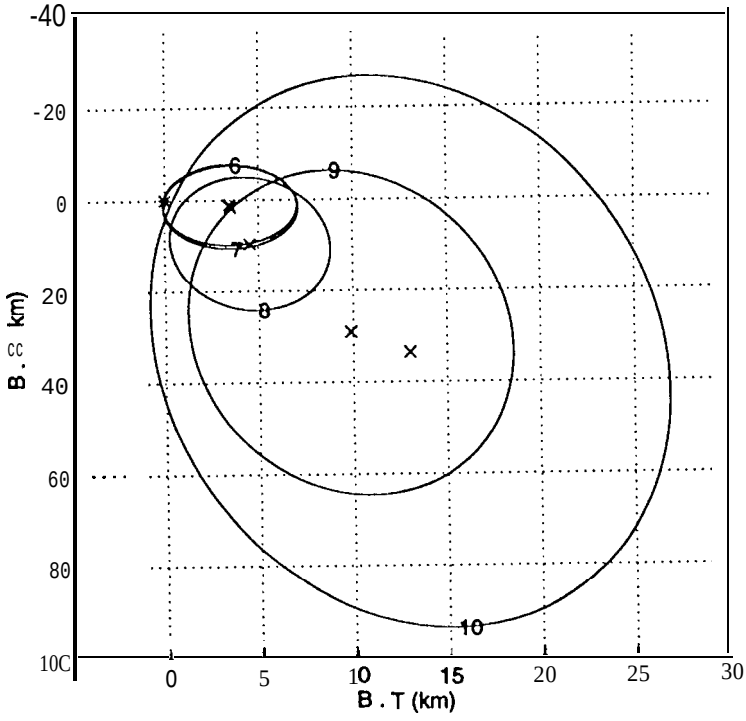

Figure 4 Encounter Results – Measurement and NGA Parameters Adapted (Range)

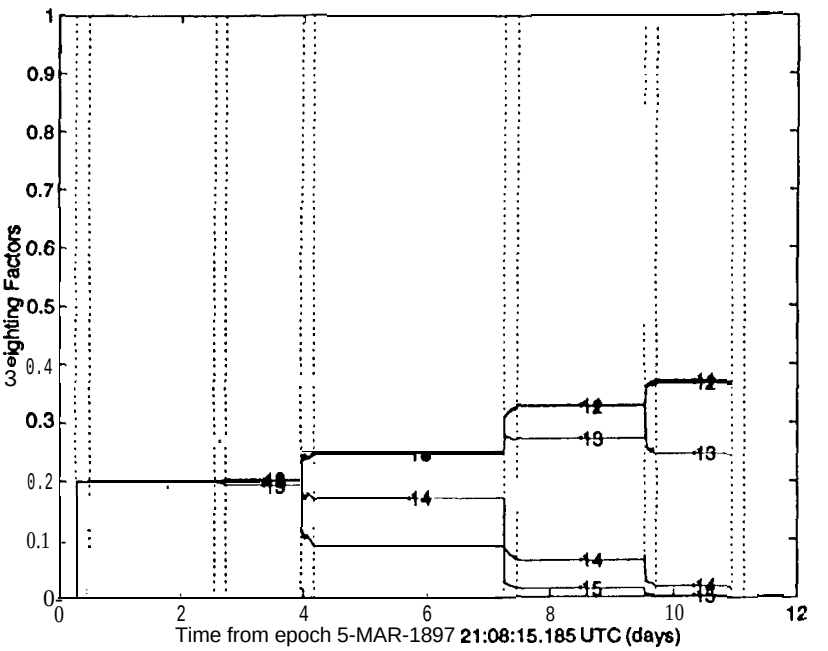

Figure 5 Weighting Coefficients – Measurement and NGA Parameters Adapted (Doppler)

Doppler Case

The Doppler case adapts the nongravitational acceleration parameters and the measurement noise parameter, A bank of 15 filters is set up with the scaling from the nominal values as shown in Table 3 for the range case.

The weighting factors for this scenario are plotted in Figure 5. This plot shows nonzero weights for filters 11 to 15, The weight for filters 11 and 12 are approximately 0.4, while filter 13 has a weight near 0.25 and filters 14 and 15 have weights of about zero. As before, the correct filter is filter 8. Thus, for this case, the filter does not converge to the correct filter. These results for the Doppler case are not as conclusive as for the range case, Problems with the formulation of the Doppler measurement due to linearization and the difference range formulation are apparent from the results. The filter chosen by the filter bank has similar or smaller process noise and larger measurement noise compared to the environment.

The encounter plane estimates and covariances for filter 8 and filters 11 through 15 are shown in Figure 6. For this case, filter 8 appears to be the best filter.

Study of Noise Parameter Variations

The final run presented involves simulated range data with a change in the nongravitational acceleration steady-state variance after approximately half of the tracking segment is complete. The parameter change represents a possible valve

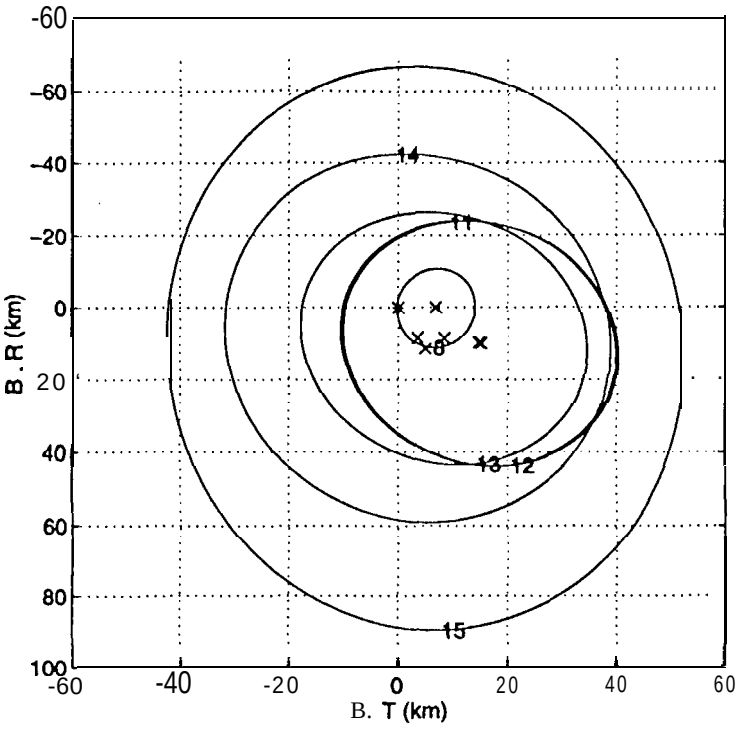

Figure 6 Encounter Results – Measurement and NGA Parameters Adapted Case (Doppler)

leak after a TCM or some other change in the force profile of the spacecraft. This variance is assumed constant for the first part of the tracking. After 62 days of tracking, or just after the Mars Pathfinder TCM 2, the parameter is changed to a new constant value. This situation represents the effect of a thruster leaking after it is fired for the TCM, a leak in a fuel line, or some other phenomena related to a thruster malfunction. The process noise term is scaled by 10, which corresponds to scaling the NGA variance by $\sqrt{10}$. The scaling was chosen to be such that the correct filter (after the variance change) is no longer part of the bank of 15 filters (see Table 3). In this way, the case will illustrate that the bank will converge to the filter operating the closest to the data's noise profile. All error sources are included in the simulation.

The weighting factors for each filter are shown in Figure 7, For the first 60 days of tracking, the filter is converging to filter 8, which is the correct filter. After the change in the variance, the filter quickly selects filter 9, which has nominal values for all variances except a scaling on the NGA of 5. It is thus shown that the bank is able to detect changes due to unmodeled thruster variations,

CONCLUSIONS

The adaptive estimation solution described in this work solves the orbit determination problem very effectively given the real-world constraints. The adaptive

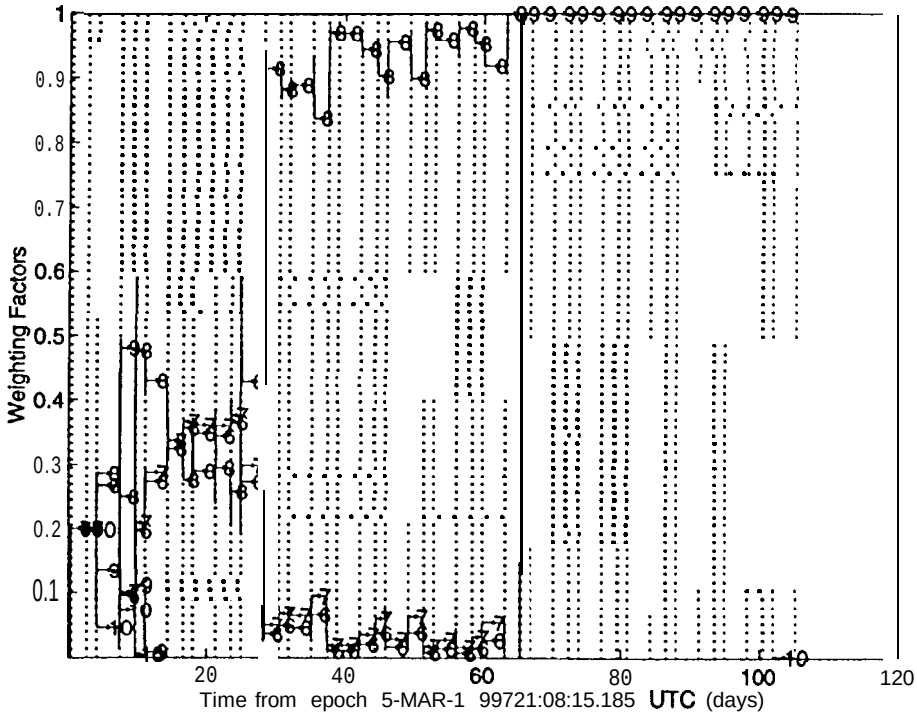

Figure 7 Weighting Coefficients – NGA Parameter Change (HGA-Range)

filter can be used as an effective tool to assist the navigation engineer in selecting filter parameters, thus allowing a closer match of the filter parameters to the true values, leading to a potentially more accurate navigation solution. In addition, this method, requires fewer hours of processing and analysis and allows a smaller group of analysts to determine accurate navigation solutions. More importantly, the long term objective of this study is to develop an adaptive filtering methodology that can be used for processing of actual mission data, It has been shown in this study that this objective is achievable.

Results for the range cases show that the Magill enhanced Kalman filter bank chooses the filter with the same parameters as the simulated data. Cases where there was no clear winner were shown to have several filters with nonzero weights and similar performance. Smaller error sources, as determined by covariance analysis, are more difficult to determine, leading to selection of no single filter, but rather several with similar performance. Based on these results, the filter bank will be a useful tooI in the tuning process for the operational filter. In addition, the bank is useful for the determination of changes in the tracking data, giving a warning of potential problems such as a thruster malfunction or some other change in the acceleration profile of the spacecraft.

Results for the Doppler cases are less conclusive. One problem with this formulation of the Doppler measurement is the effect of roundoff errors due to the linearization and the difference range formula. For example, the range values are on the order of 10^8 km. The measurement noise on the Doppler measurement is 0.01 mm/s, or 10^{-8} km. The difference is 16 digits, or near the numerical limits of a 64 bit number. In addition, the difference range formulation implemented in the partial derivatives and the data generation may be susceptible to differences due to Earth rotation from the start to the end of the tracking pass. One way to address these problems is to implement a more theoretically correct version of the range rate measurement. In addition, an extended Kalman filter, which does not involve a linearization about a reference trajectory, may help this problem as well. The Doppler results in general show that filters with larger measurement noise are chosen, while the other filters have zero weights. In most cases, the filters with correct or smaller process noise are chosen, as for the range case.

A next step is implementation of the filter bank for use in processing actual mission data. The proposed method could be used by the navigation team members making the individual runs to systematically eliminate incorrect filter models. This could be completed by several individuals independently, with comparison of results after processing is complete. The development of an extended Kalman filter capable of processing real data is under way, and the Mars Pathfinder problem will be one of the first cases tested.

One additional advantage is the obvious parallel computing possibilities with this approach. This approach can be implemented using search methods (such as genetic algorithms[21]) to update the filter bank for operation in an iterative fashion. These genetic algorithms can be implemented easily using the filter bank and can

be implemented in a parallel processing environment[22].

The Kalman filter bank is a method that has a successful history in real-time applications such as power system fault detection, image processing and terrain-height correlation for helicopter navigation. It has been shown here to also have application in interplanetary orbit determination.

ACKNOWLEDGEMENTS

The authors would like to thank Jeff Estefan, Vincent Pollmeier, Dr. Sam Thurman and Dr. Lincoln Wood of the Jet Propulsion Laboratory for their contributions to this study. The work described in this paper was performed at The University of Texas at Austin and the Jet Propulsion Laboratory, California Institute of Technology, under a contract from the National Aeronautics and Space Administration.

REFERENCES

1. Estefan, J. A., Pollmeier, V. M. and Thurman, S. W., "Precision X-Band Doppler and Ranging Navigation for Current and Future Mars Exploration Missions," *Advances in the Astronautical Sciences,* J. Teles and M. V. Samii, Editors, Vol. 84, Part I, pp. 3-16, 1993.

2. Bhaskaran, S., Thurman, S. W. and Pollmeier, V. M., "Demonstration of a Precision Data Reduction Technique for Navigation of the Galileo Spacecraft", *Advances in the Astronautical Sciences,* J. E. Cochran et al., Editors, Vol. 87, Part II, pp. 785-798, 1994.

3. Magill, D. T., "Optimal Adaptive Estimation of Sampled Stochastic Processes," *IEEE Transactions on Automatic Control,* Vol AC-10, No. 4, October, 1965, pp. 434-439.

4. Kallemeyn, P., "Pathfinder Project Navigation Plan - Critical Design Review Version," *JPL* Document *D-11349* (Internal Document), July, 1994.

5. Gelb, A., *Applied Optimal Estimation,* MIT Press, 1974.

6. Bierman, G. J., *Factorization Methods for Discrete Sequential Estimation,* Academic Press, 1977.

7. Jordan, James F., Madrid, George A. and Pease, Gerald E., "Effects of Major Error Sources on Planetary Spacecraft Navigation Accuracies", *Journal of Spacecraft and Rockets,* Vol. 9, No. 3, March, 1972, pp. 196-204.

8. Kizner, W., "A Method of Describing Miss Distances for Lunar and Interplanetary Trajectories," *JPL External Publication No. 674,* August 1, 1959.

9. Burkhart, P. D., Bishop, R.H. and Estefan, J. A, "Covariance Analysis of Mars Pathfinder Interplanetary Cruise", *Advances in the Astronautical Sciences,* H. Jacobs, Series Editor, Vol. 89, 1995.

10. Mehra, Raman K., "Approaches to Adaptive Filtering," *IEEE Transactions on Automatic Control*, October, 1972, pp. 693-698.

11. Burkhart, P. D., "Adaptive Orbit Determination for Interplanetary Spacecraft," Ph.D. Dissertation, The University of Texas at Austin, May, 1995.

12. Meyers, Kenneth A. and Tapley, Byron D., "Adaptive Sequential Estimation with Unknown Noise Statistics," *IEEE Transactions on Automatic Control*, August, 1976, pp. 520-523.

13. Mehra, Raman K., "On the Identification of Variances and Adaptive Kalman Filtering," *IEEE Transactions on Automatic Control*, Vol. AC-15, No. 2, April, 1970, pp. 175-184.

14. Bélanger, Pierre R., "Estimation of Noise Covariance Matrices for a Linear Time-Varying Stochastic Process," *Automatica*, Vol. 10, May, 1974, pp. 267-275.

15. Brown, Robert G. and Huang, Patric Y. C., *Introduction to Random Signals and Applied Kalman Filtering*, Second Edition, John Wiley and Sons, 1992, pp. 398-402.

16. Brown, R. G., "A New Look at the Magill Adaptive Filter as a Practical Means of Multiple Hypothesis Testing," *IEEE Transactions on Circuits and Systems*, Vol CAS-30, No. 10, October, 1983, pp. 765-768.

17. Brown, R. G. and Hwang, P. Y. C., "A Kalman Filter Approach to Precision GPS Geodesy," *Navigation, Journal of the Institute of Navigation, 30:, No.* 4, Winter 1983-84, pp. 338-349.

18. Mealy, G. L., "Application of Multiple Model Estimation to a Recursive Terrain Height Correlation System," *IEEE Transactions on Automatic Control*, Vol. AC-28, No. 3, March, 1983, pp. 323-331.

19. Girgis, A. A. and Brown, R. G., "Adaptive Kalman Filtering in Computer Relaying: Fault Classification using Voltage Models," *IEEE Transactions on Power Apparatus and Systems*, Vol. PAS-104, No. 5, May, 1985, pp. 1168-1177.

20. Hilborn, C. G., Jr. and Lainiotis, D. G., "Optimal Adaptive Filter Realizations for Sample Stochastic Processes with an Unknown Parameter," *IEEE Transactions on Automatic Control*, Vol AC-14, December, 1969, pp. 767-770.

21. Goldberg, D. E., *Genetic Algorithms in Search, Optimization, and Machine Learning*, Addison-Wesley, 1989

22. Chaer, W. S. and Bishop, R. H., "Adaptive Kalman Filtering with Genetic Algorithms," *Advances in the Astronautical Sciences*, H. Jacobs, Series Editor, Vol. 89, 1995.